SPECTRAL ANALYSIS OF IRREGULARLY SAMPLED DATA USING A BERNOULLI-GAUSSIAN MODEL WITH FREE FREQUENCIES

Sébastien Bourguignon, Hervé Carfantan

Laboratoire d'Astrophysique de l'Observatoire Midi-Pyrénées, Université Paul Sabatier - Toulouse III
14, avenue Édouard Belin, 31400 Toulouse, France
bourgui@ast.obs-mip.fr, Herve.Carfantan@obs-mip.fr

ABSTRACT

Line spectra estimation is addressed for irregularly sampled astrophysical data. A formulation with a large number of discretized frequencies is used and sparseness is encouraged via a Bernoulli-Gaussian (BG) model on the corresponding amplitudes. Contrary to classic BG models, here the frequency parameters are not constrained on a fixed grid, theoretically enabling unlimited frequency precision. We propose a posterior mean unsupervised estimation scheme combined with an hybrid MCMC algorithm, that allows us to derive crucial information in an astrophysical context, such as confidence levels and variances for each detected spectral line. Simulations confirm the validity of this model with satisfactory estimation results, in addition to a more solid behaviour than parametric methods towards classic astrophysical perturbations.

1. INTRODUCTION

The search for periodicities in astronomical time series has a wide field of applications. In asteroseismology, the detection of spectral lines from radial velocity or light curves allows us to identify the pulsation modes of variable stars. It is also the key tool for studying multiple systems and for indirectly detecting exoplanets. Astronomical data generally suffer irregular sampling and additional periodic gaps may appear due to the day/night and seasonal alternations causing the periodic invisibility of the object. The Fourier spectrum is thus ineffective for detecting spectral lines, and sampling irregularities render many classical methods unapplicable. Furthermore, approximately one of two stars is part of a multiple system, where the relatively slow orbital movement may cause low frequency variations dominating the data and perturbating the estimation of lines at higher frequencies, as shown in Fig. 1.

High resolution spectral analysis has recently been addressed as a linear inverse problem. A non parametric model of data $\boldsymbol{y} = [y(t_1), \dots y(t_n)]^T$ is used with an arbitrarily large number of sinusoids with discretized frequencies on the grid $\mathcal{G} = \{f_k^{\mathcal{G}}\}_{k=0\dots P} \triangleq \{\frac{k}{P} f_{\max}\}_{k=0\dots P}$:

$$\mathcal{M}_{\mathcal{G}} : y(t_n) = \sum_{k=0}^{P} a_k \cos 2\pi f_k^{\mathcal{G}} t_n + b_k \sin 2\pi f_k^{\mathcal{G}} t_n + \epsilon_n.$$

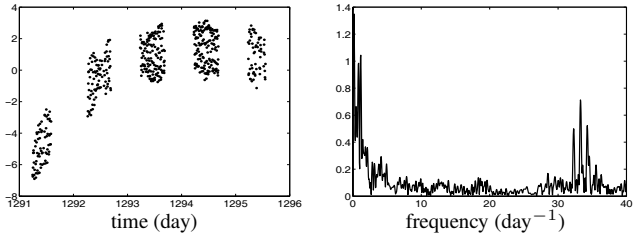

Fig. 1. Left: radial velocity curve of star HD 104237 for five observing nights. Right: its Fourier spectrum. Several spectral lines are expected around 33 day^{-1} but only one peak is retrieved with its 1 day^{-1} sidelobes.

Line spectrum estimation is then addressed by reconstructing a *sparse* vector of amplitudes through some regularization. Such a formulation can be used for every sampling scheme contrary to many parametric methods that require even sampling. Although this model is not strictly adapted to low frequency perturbations as shown in Fig. 1, it also revealed the ability [1] to retrieve high frequency spectral lines from these raw data where multi-sinusoidal models [2] cannot be fitted. The first paper by Sacchi *et al.* [3] introduces the model $\mathcal{M}_{\mathcal{G}}$ via Tikhonov regularization by minimizing an adequately penalized least-squares criterion. A Bernoulli-Gaussian probabilistic model on the spectral amplitudes has been proposed by bayesian maximum *a posteriori* (MAP) estimation [4] that showed satifactory results but also exhibited limitations due to a necessary supervised and suboptimal optimization. An alternative proposed by Cheng *et al.* [5] for Bernoulli-Gaussian deconvolution makes use of Markov Chain Monte-Carlo methods (MCMC) to perform an unsupervised posterior mean (PM) estimation. It was successfully adapted to the spectral analysis problem for model $\mathcal{M}_{\mathcal{G}}$ [1], where this strategy allows us to derive essential information in terms of confidence levels and variances associated to the detected spectral lines.

However, model $\mathcal{M}_{\mathcal{G}}$ is intrinsically limited by the discretization constraint on a *fixed* frequency grid, and reducing the grid step substantially increases the computational cost. In [4] an extended BG model is proposed to improve the frequency precision. The problem was addressed through MAP estimation which provided only partial satisfaction due to the increased complexity of the optimization problem. To our

knowledge this extension has not been utilized since then, although it enables the localization of the frequency parameters (or the spike trains for BG deconvolution) on a *continuous* set. In this paper, we propose a PM estimation scheme through an hybrid MCMC algorithm for such a model.

2. MODEL DESCRIPTION AND ESTIMATION

2.1. An extended Bernoulli-Gaussian model

We consider the extension of model $\mathcal{M}_{\mathcal{G}}$ where the frequencies now belong to continuous spectral bands $\mathcal{I}_k = [f_{k-1}^{\mathcal{G}}, f_k^{\mathcal{G}}]$:

$$\mathcal{M}_{\boldsymbol{df}} : y(t_n) = \sum_{k=0}^{P} a_k \cos 2\pi f_k t_n + b_k \sin 2\pi f_k t_n + \epsilon_n$$

where $f_0 = 0$ and $\forall k \geq 1, f_k = f_k^{\mathcal{G}} - df_k,\ df_k \in [0, \frac{f_{\max}}{P}]$.

Introducing $\boldsymbol{s}_k = [a_k, b_k]$ and the $2P+2$ amplitude vector $\boldsymbol{s} = [\boldsymbol{s}_0, \ldots, \boldsymbol{s}_P]^T$, model $\mathcal{M}_{\boldsymbol{df}}$ writes equivalently:

$$\boldsymbol{y} = \mathbf{H}_{\text{df}} \boldsymbol{s} + \epsilon \tag{1}$$

where $\mathbf{H}_{\text{df}_{n,2k}} = \cos 2\pi(f_k^{\mathcal{G}} - df_k)t_n$, $\mathbf{H}_{\text{df}_{n,2k+1}} = \sin 2\pi(f_k^{\mathcal{G}} - df_k)t_n$ and $\boldsymbol{\epsilon}$ stands for perturbations such as additive noise and model errors. Here $\boldsymbol{\epsilon}$ is supposed centered, white and gaussian with variance σ_ϵ^2. Irregular sampling makes the alias-free frequency range much wider than with regular sampling [6]: there is no Nyquist limit and the maximum frequency $f_{\max}$ of the model is set according to physical prior information.

As only a few lines are searched, we introduce the following probabilistic model similarly to [4]:

- a white Bernoulli sequence $\boldsymbol{q} = [q_0, \ldots, q_P]^T$ is defined to control the sparsity of the solution: $\Pr(q_k = 1) = \lambda$ is the prior probability of existence of a spectral line in the spectral band $\mathcal{I}_k$;
- the frequency shifts $df_{k,\, k=1\ldots P}$ are considered independent and uniformly distributed in $\Delta f \triangleq [0, \frac{f_{\max}}{P}]$;
- conditionally to the localization by the Bernoulli variables, amplitudes $(a_k \,|\, q_k = 1)$ and $(b_k \,|\, q_k = 1)$ of the spectral line in $\mathcal{I}_k$ are centered gaussian variables with variance σ^2: $p(\boldsymbol{s}_k | q_k) = g_2(\boldsymbol{s}_k, q_k\sigma^2\mathbf{I}_2)$, where g_m stands for the m-variate centered gaussian distribution:
$$g_m(\boldsymbol{x}, \Sigma) = \frac{1}{(2\pi)^{N/2}|\Sigma|^{1/2}} e^{-\frac{1}{2}\boldsymbol{x}^T\Sigma^{-1}\boldsymbol{x}}.$$
The case $q_k = 0$ corresponds to an improper centered gaussian distribution with a zero covariance matrix, *i.e.,* a Dirac distribution $\delta_2(\boldsymbol{s}_k)$.

Independence between $\boldsymbol{df}$ and $\boldsymbol{s}$ in the above definition is utilized for practical convenience. Obviously, the frequency shifts df_k are only meaningful when $q_k = 1$; this will be considered in the posterior estimation procedure.

The estimation of the unknown quantities $\boldsymbol{q}, \boldsymbol{s}$ and $\boldsymbol{df}$ in $\mathcal{M}_{\boldsymbol{df}}$ is a quite more complex problem than simply estimating $\boldsymbol{q}, \boldsymbol{s}$ in $\mathcal{M}_{\mathcal{G}}$ because of the non-linearity in new parameters $\boldsymbol{df}$. A MAP strategy was proposed [4] by a combinatorial exploration algorithm similar to the classic suboptimal SMLR procedure introduced in BG deconvolution [7]. To cope with non-linearities, however, several approximation levels were necessary (first-order linearization of model $\mathcal{M}_{\boldsymbol{df}}$, gaussian approximation of the unusable integral exponential distribution) that provided only partial satisfaction. We consider here a PM estimation combined with a stochastic sampling algorithm. Such a strategy enables the joint estimation of $(\boldsymbol{q}, \boldsymbol{s})$ and $\boldsymbol{df}$ in a unified procedure while providing additional variance estimation on each parameter, which is essential information not accessible by MAP estimation.

2.2. Unsupervised procedure

Fully unsupervised estimation can furthermore be addressed by jointly sampling and estimating $\boldsymbol{q}, \boldsymbol{s}, \boldsymbol{df}$ and $\boldsymbol{\theta}$ from the posterior distribution $p(\boldsymbol{q}, \boldsymbol{s}, \boldsymbol{df}, \boldsymbol{\theta} | \boldsymbol{y}) \propto p(\boldsymbol{q}, \boldsymbol{s}, \boldsymbol{df} | \boldsymbol{y}, \boldsymbol{\theta}) p(\boldsymbol{\theta})$. With appropriate priors $p(\boldsymbol{\theta})$ on the hyperparameters, the global computational cost of the sampling procedure is nearly left unchanged. We consider a uniform prior on the Bernoulli parameter λ and Jeffreys' uninformative (improper) priors [8] on the variances: $p(\sigma^2) \propto \sigma^{-2}$, $p(\sigma_\epsilon^2) \propto \sigma_\epsilon^{-2}$. Such choices do not require the adjustment of any additional parameter and guarantee the integrability of $p(\boldsymbol{q}, \boldsymbol{s}, \boldsymbol{df} | \boldsymbol{y}, \boldsymbol{\theta}) p(\boldsymbol{\theta})$ *w.r.t.* $\boldsymbol{\theta}$, which is necessary to sample properly from the joint distribution $p(\boldsymbol{q}, \boldsymbol{s}, \boldsymbol{df}, \boldsymbol{\theta} | \boldsymbol{y})$ [8]. The latter writes by Bayes' rule:

$$\begin{aligned} p(\boldsymbol{q}, \boldsymbol{s}, \boldsymbol{df}, \boldsymbol{\theta} | \boldsymbol{y}) \quad &\propto \quad p(\boldsymbol{y} | \boldsymbol{q}, \boldsymbol{s}, \boldsymbol{\theta})\, p(\boldsymbol{q}, \boldsymbol{s}, \boldsymbol{df} | \boldsymbol{\theta}) p(\boldsymbol{\theta}) \\ &\propto \quad g_N(\boldsymbol{y} - \mathbf{H}_{\text{df}}\, \boldsymbol{s},\ \sigma_\epsilon^2 \mathbf{I}_N) \\ &\quad \times \prod_{k=0}^{P} \left(\lambda g_2(\boldsymbol{s}_k, \sigma^2 \mathbf{I}_2) + (1-\lambda)\delta_2(\boldsymbol{s}_k)\right) \\ &\quad \times \prod_{k=1}^{P} \mathbf{1}_{\Delta f}\,(df_k) \times \sigma^{-2}\sigma_\epsilon^{-2}. \end{aligned} \tag{2}$$

2.3. Estimation strategy

Suppose that samples $(\boldsymbol{q}^{(u)}, \boldsymbol{s}^{(u)}, \boldsymbol{df}^{(u)}, \boldsymbol{\theta}^{(u)})_{u=1\ldots U}$ are drawn according to (2). We propose the following estimation scheme.

1. First, estimate the posterior mean of the Bernoulli sequence: $\widehat{\boldsymbol{q}}_{\text{PM}} = \frac{1}{U}\sum_u \boldsymbol{q}^{(u)}$ and of the hyperparameters: $\widehat{\boldsymbol{\theta}}_{\text{PM}} = \frac{1}{U}\sum_u \boldsymbol{\theta}^{(u)}$. Then, perform the *detection* step by suitably thresholding $\widehat{\boldsymbol{q}}_{\text{PM}}$ and build the corresponding Bernoulli sequence $\widehat{\boldsymbol{q}}_\alpha$: $\widehat{\boldsymbol{q}}_{\alpha_k} = 1$ if $\widehat{\boldsymbol{q}}_{\text{PM}_k} > \alpha$.
2. Estimate the conditional posterior mean of the frequency shifts $\mathbb{E}[\boldsymbol{df} | \boldsymbol{y}, \boldsymbol{q} = \widehat{\boldsymbol{q}}_\alpha]$ and their variances. That is:
$$\begin{aligned} \text{for } k/\widehat{\boldsymbol{q}}_{\alpha_k} = 1,\ \widehat{df_k} \quad &= \quad \frac{1}{U_\alpha} \sum_{u\,|\boldsymbol{q}^{(u)} = \widehat{\boldsymbol{q}}_\alpha} df_k^{(u)} \\ \text{and var } \widehat{df_k} \quad &\simeq \quad \frac{1}{U_\alpha - 1} \sum_{u\,|\boldsymbol{q}^{(u)} = \widehat{\boldsymbol{q}}_\alpha} (df_k^{(u)} - \widehat{df_k})^2 \end{aligned}$$
where $U_\alpha = \text{Card}\{u \,|\, \boldsymbol{q}^{(u)} = \widehat{\boldsymbol{q}}_\alpha\}$.

3. Finally perform the PM estimation of the conditional amplitudes $\mathbb{E}[\boldsymbol{s}|\boldsymbol{q} = \widehat{\boldsymbol{q}}_\alpha, \widehat{\boldsymbol{df}}]$ and their variances. Under the gaussian assumptions on the priors $p(\boldsymbol{s}|\boldsymbol{q})$ and the noise distribution, both quantities have explicit analytical expressions as functions of $\boldsymbol{y}$, $\widehat{\boldsymbol{q}}_\alpha$, $\widehat{\boldsymbol{df}}$ and $\widehat{\boldsymbol{\theta}}_{\text{PM}}$.

Step 1 associates by means of $\widehat{\boldsymbol{q}}_{\text{PM}_k}$ a posterior probability to the possible detection of a spectral line in every band $\mathcal{I}_k$ and threshold α corresponds to a minimum *confidence level* for each detection. Complementary variance estimation in steps 2 and 3 also gives additional precision on the estimated parameters. This strategy appears similar to the estimation of multiple sinusoids proposed by [2] for a Poisson-Gaussian (PG) prior using a reversible jump MCMC algorithm. The main difference is in the detection step: in [2] a posterior probability is assigned to the model *order* whereas in our approach a probability is assigned independently to the possible detection of a spectral line in each of the P spectral bands $\mathcal{I}_k$. Simulations in section 4 will show that our strategy also brings more robustness towards modelling errors.

3. AN HYBRID ALGORITHM

We describe an MCMC algorithm to draw samples from the joint posterior distribution (2). Note that the integration of amplitude parameters $\boldsymbol{s}$ leads to an explicit marginal density. Sampling from the marginal $p(\boldsymbol{q}, \boldsymbol{df}, \boldsymbol{\theta}|\boldsymbol{y})$, however, is much more burdensome than sampling from (2) and leads to a less efficient procedure. Let $p(\boldsymbol{x}|-)$ denote the posterior conditional distribution of random variable $\boldsymbol{x}$ where « – » represents all other random variables and the data $\boldsymbol{y}$. The Gibbs sampler is an appropriate algorithm for sampling the parameters of model $\mathcal{M}_{\mathcal{G}}$ as the conditional variables $(\boldsymbol{q}_k, \boldsymbol{s}_k|-)$ follow BG distributions [5] and $p(\theta_k|-)$ belong to classical distributions. While such properties still hold for $(\boldsymbol{q}_k, \boldsymbol{s}_k)$ and θ_k when extending to model $\mathcal{M}_{\boldsymbol{df}}$, the conditional distributions of the frequency shifts write:

$$p(df_k|-) \propto \exp\left(-\frac{\|\boldsymbol{e}_k - \mathbf{H}_{\text{df}_k}\boldsymbol{s}_k\|^2}{2\sigma_\epsilon^2}\right) \times \mathbf{1}_{\Delta f}(df_k) \quad (3)$$

where $\mathbf{H}_{\text{df}_k}$ is the $N \times 2$ matrix formed by the $2k$ and $2k+1$ columns of matrix $\mathbf{H}_{\text{df}}$ and $\boldsymbol{e}_k = \boldsymbol{y} - \sum_{\ell \neq k} \mathbf{H}_{\text{df}_\ell}\boldsymbol{s}_\ell$. As direct sampling from (3) is not possible, we perform a Metropolis-Hastings (MH) step with (3) as equilibrium distribution: at iteration t, a candidate df_k is drawn according to a proposal $\phi(df_k|df_k^{(u-1)})$ and accepted with probability:

$$\rho = \min\left\{1, \frac{p(df_k\,|-)}{p(df_k^{(u-1)}\,|-)} \frac{\phi(df_k^{(u-1)}\,|\,df_k)}{\phi(df_k\,|\,df_k^{(u-1)})}\right\}.$$

Following [2], we mix two proposal distributions: $\phi_1(df_k)$ is a uniform distribution on Δf and $\phi_2(df_k|df_k^{(u-1)})$ is a gaussian random walk truncated to Δf enabling a local exploration of the posterior (3). Samples of ϕ_2 are drawn by simulating the untruncated gaussian law until the sample belongs to Δf: this can be viewed as an acceptation-rejection procedure [8] where a small variance of the random walk ensures a high acceptation rate. Here the corresponding standard deviation is set to 10% the size of Δf.

As proposals are symmetric, the expression of probability ρ reduces to the posterior ratio. Algorithm is given in Tab. 1.

- For $k = 0 \ldots P$: (i) sample $(q_k, \boldsymbol{s}_k)$ according to:

  $$p(q_k, \boldsymbol{s}_k|-) = \lambda_k g_2(\boldsymbol{s}_k - \boldsymbol{\mu}_k, \mathbf{R}_k) + (1-\lambda_k)\delta_2(\boldsymbol{s}_k)$$
  $$\text{with } \lambda_k = \frac{\widetilde{\lambda}_k}{\widetilde{\lambda}_k + (1-\lambda)}, \widetilde{\lambda}_k = \frac{\lambda}{\sigma^2}|\mathbf{R}_k|^{1/2} e^{\boldsymbol{\mu}_k^T \mathbf{R}_k^{-1} \boldsymbol{\mu}_k},$$
  $$\mathbf{R}_k^{-1} = \tfrac{\mathbf{I}_2}{\sigma^2} + \tfrac{1}{\sigma_\epsilon^2}\mathbf{H}_{\text{df}_k}^T\mathbf{H}_{\text{df}_k}, \quad \boldsymbol{\mu}_k = \tfrac{1}{\sigma_\epsilon^2}\mathbf{R}_k\mathbf{H}_{\text{df}_k}^T\boldsymbol{e}_k.$$

  (ii) if $k \geq 1$, perform a MH step with invariant distribution $p(df_k|-)$ given by (3): sample $u \sim \mathcal{U}_{[0,1]}$ and use proposal ϕ_1 if $u < 1/2$, else use proposal ϕ_2.

- Sample the hyperparameters according to their conditional posterior distributions:

  $$(\lambda|-) \sim \mathcal{B}e(M_q + 1, P + 1 - M_q)$$
  $$(\sigma^2|-) \sim \begin{cases}\mathcal{IG}(M_q + 1, ||\boldsymbol{s}||^2/2) \text{ if } \boldsymbol{s}_0 = \boldsymbol{0} \\ \mathcal{IG}(M_q + 1/2, ||\boldsymbol{s}||^2/2) \text{ else}\end{cases}$$
  $$(\sigma_\epsilon^2|-) \sim \mathcal{IG}(N/2 + 1, ||\boldsymbol{y} - \mathbf{H}_{\text{df}}\boldsymbol{s}||^2/2)$$

  where M_q is the number of non zero components in the sequence $\boldsymbol{q}$, $\mathcal{B}e$ and $\mathcal{IG}$ stand for the beta and inverse-gamma distributions, respectively.

Table 1. Hybrid MCMC algorithm for $\mathcal{M}_{\boldsymbol{df}}$.

This scheme generates the frequency shifts df_k conditionally to the value of the amplitudes $\boldsymbol{s}_k$, whereas the inverse procedure may appear more natural. Recall, however, that amplitude sampling is introduced because jointly sampling $(q_k, \boldsymbol{s}_k|-)$ is computationally more efficient than sampling the conditionals $(q_k|-)$ from the marginal distribution. The only drawback to this approach is that the MH step may reject too many candidates df_k if the fixed amplitude $\boldsymbol{s}_k$ is not appropriate, which would slow down the convergence of the chain. With sufficiently small spectral bands $\mathcal{I}_k$, however – *i.e.,* with P sufficiently large – one can expect the amplitude that best models a spectral line in $\mathcal{I}_k$ to depend slightly on the exact localization of the frequency in $\mathcal{I}_k$. In practice, satisfactory acceptation rates were obtained.

4. SIMULATION RESULTS

The signal shown in Fig. 2 is the sum of 5 sinusoids with frequencies from 0.1 to 0.16 day^{-1} with 5 dB white gaussian noise. The 250 points are unvenly sampled with additional periodic gaps and the Fourier spectrum is unreadable. Posterior mean $\widehat{\boldsymbol{q}}_{\text{PM}}$ shown in Fig. 3 was obtained after 5000 iterations of algorithm in section 3, where the first 1000 samples were discarded to remove initialization effects. A $P = 100$ point grid was used with $f_{\max} = 0.25$ day^{-1}. The spectral lines are localized in the correct spectral bands with the highest confidence level: in this example $\widehat{\boldsymbol{q}}_{\text{PM}}$ equals to 1 at the 5 correct

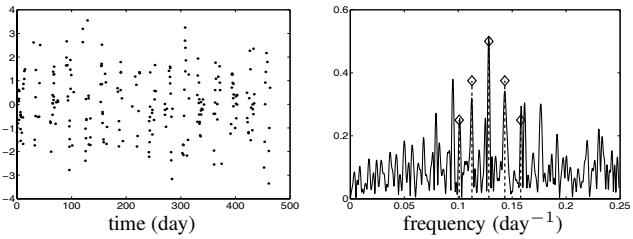

Fig. 2. Left: irregularly sampled multi-sinusoidal signal. Right: Fourier spectrum (–) and true lines (⋄).

locations while it takes small values elsewhere. Accurate estimations of the corresponding frequencies $\widehat{f_i}$ and amplitudes are obtained. Due to lack of space, we focus above all on the frequency estimation, which is the crucial point. In this example the grid precision equals $f_{\max}/P = 2.5 \times 10^{-3}$ day^{-1} whereas the mean frequency error is 1.16×10^{-4} day^{-1}.

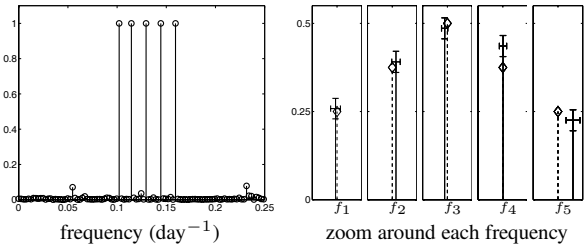

Fig. 3. Left: estimate $\widehat{\boldsymbol{q}}_{\text{PM}}$. Right: posterior estimation for each detected line. Errorbars correspond to standard deviations, ⋄ to the true values. Bandwidth around each frequency is $f_{\max}/2P$ (half the grid precision).

A comparison is given with the estimator – denoted PG – proposed by [2] that also provides variance information on each detected spectral line and can be adapted to irregular sampling. In this case, however, the use of the Fourier spectrum to build a convenient proposal in the MH algorithm can be critical; here a uniform proposal was used instead. Tab. 2 shows similar performances of both estimators and the mean frequency error for PG is 1.27×10^{-4} day^{-1}. However, PG only provides a probability on the model order (in this case 85% of the samples correspond to the correct order 5) whereas model $\mathcal{M}_{\boldsymbol{df}}$ allows a more complete posterior interpretation for every spectral band.

	$\mathcal{M}_{\boldsymbol{df}}$			PG	
	$\lvert\widehat{f_i} - f_i\rvert$ $\times 10^{-4}$ d^{-1}	std$\widehat{f_i}$ $\times 10^{-4}$ d^{-1}	$\widehat{\boldsymbol{q}}_{\text{PM}}$	$\lvert\widehat{f_i} - f_i\rvert$ $\times 10^{-4}$ d^{-1}	std$\widehat{f_i}$ $\times 10^{-4}$ day^{-1}
f_1	0.4	1.2	1	0.4	1.5
f_2	0.9	1.1	1	1.4	1.0
f_3	0.7	0.8	1	0.6	0.8
f_4	0.0	0.9	1	0.3	0.1
f_5	3.8	1.8	1	3.7	1.8

Table 2. Estimation results compared to PG estimation [2].

We finally show that estimation provided by model $\mathcal{M}_{\boldsymbol{df}}$ is robust when data present typical low-frequency perturbations as in Fig. 1. A signal is simulated based on the same sampling scheme and orbital movement as in Fig. 1 with four spectral lines with frequencies between 28 and 25 day^{-1}. No satisfactory result was obtained by parametric approaches as PG or astrophysical CLEAN deconvolution methods. Estimation with $\mathcal{M}_{\boldsymbol{df}}$ shown in Fig. 4 achieves a satisfactory estimation: $\widehat{\boldsymbol{q}}_{\text{PM}}$ is almost 1 at low frequencies but also at the locations of the four true lines, and the corresponding parameters are correctly estimated. In this example, the mean frequency error is 6×10^{-3} day^{-1}. Note that a thinner grid (P=500) was used to account for the low-frequency continuous spectrum by a sufficient number of frequency components. A higher number of iterations was also necessary, resulting in a considerable increase of the computational burden.

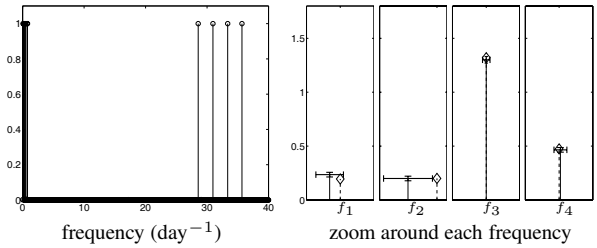

Fig. 4. Results on a low-frequency perturbated signal. Left: estimate $\widehat{\boldsymbol{q}}_{\text{PM}}$. Right: posterior estimation for each detected line. Errorbars correspond to standard deviations, ⋄ to the true values. Bandwidth around each frequency is half the grid precision, *i.e.,* $f_{\max}/2P = 0.04$ day^{-1}.

5. REFERENCES

[1] S. Bourguignon and H. Carfantan, "Bernoulli-Gaussian spectral analysis of unevenly spaced astrophysical data," in *IEEE 13th workshop on Statistical Signal Processing*, Paper #238, Bordeaux, France, July 2005.

[2] C. Andrieu and A. Doucet, "Joint bayesian model selection and estimation of noisy sinusoids via reversible jump MCMC," *IEEE Transactions on Signal Processing*, vol. 47, no. 10, pp. 2667–2676, Oct. 1999.

[3] M.D. Sacchi, T.J. Ulrych, and C.J. Walker, "Interpolation and extrapolation using a high-resolution discrete Fourier transform," *IEEE Transactions on Signal Processing*, vol. 46, no. 1, pp. 31–38, Jan. 1998.

[4] F. Dublanchet, *Contribution de la méthodologie bayésienne à l'analyse spectrale de raies pures et à la goniométrie haute résolution*, Ph.D. thesis, Université de Paris-Sud, Oct. 1996.

[5] Q. Cheng, R. Chen, and T.-H. Li, "Simultaneous wavelet estimation and deconvolution of reflection seismic signals," *IEEE Transactions on Geoscience and Remote Sensing*, vol. 34, no. 2, pp. 377–384, Mar. 1996.

[6] L. Eyer and P. Bartholdi, "Variable stars: which Nyquist frequency?," *Astronomy and Astrophysics Supplement Series*, vol. 135, pp. 1–3, Feb. 1999.

[7] J. Kormylo and J.M. Mendel, "Maximum-likelihood detection and estimation of Bernoulli-Gaussian processes," *IEEE Transactions on Information Theory*, vol. 28, pp. 482–488, 1982.

[8] C. Robert, *Méthodes de Monte-Carlo par Chaînes de Markov*, Economica, Paris, 1996.